Stopping, heating, thermalization and expansion at SPS energies

Jens Jørgen Gaardhøje
Niels Bohr Institute, Blegdamsvej 17, 2100 Copenhagen, Denmark

1 Introduction.

The Pb beam at $158AGeV$ from the CERN SPS accelerator which was taken into use in the fall of 1994 has opened a new dimension in the study of highly excited nuclear matter in heavy ion reactions. It has now become possible to form reasonably large volumes (containing more than 300 nucleons) in central collisions between heavy ions, with energy and matter densities in some parts of the volume exceeding those expected for the phase transition from hadronic matter to deconfined quark and gluon matter. In this talk we discuss some features of the expansion of the hot and compressed system that may be learned by analysing the single particle spectra of baryons and mesons with emphasis on data from the NA44 experiment.

2 The Na44 experiment.

The NA44 experiment which has been operating at the CERN SPS accelerator is schematically shown in figure 1. The instrument consists of two sections: a magnetic spectrometer that accepts particles originating from the target in a 3 mstr opening and which focusses them into nearly parallel trajectories and a detector section able to fully identify charged hadrons. The magnetic spectrometer consists of two dipole magnets and 3 superconducting quadrupoles. The detector section contains a number of tracking devices (Si pad and drift chambers),

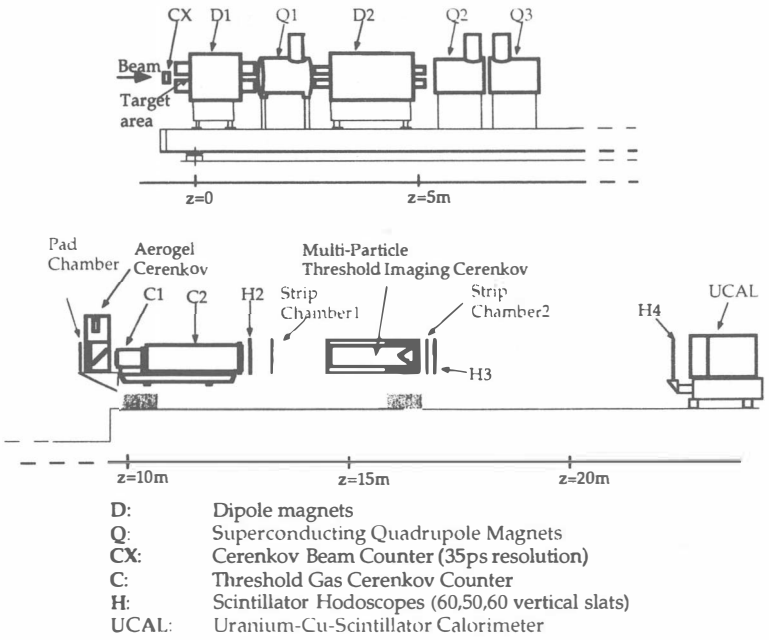

Figure 1: The NA44 (focussing) spectrometer at the CERN SPS accelerator.

segmented time of flight hodoscopes (H2, H3 and H4), gas Cerenkov theshold counters (C1, C2 and TIC), and a Uranium/scintillator calorimeter (UCAL). Global event characterization (centrality) is done with two plastic scintillators that record total charged particle energy and a circular Si drift detector segmented into 256 sections. The time reference is supplied by a thin gas Cerenkov beam counter located upstream of the target with an intrinsic time resolution of 35 ps.

The acceptance of the NA44 spectrometer for various hadron species is shown in figure 2. For Pb + Pb reactions the spectrometer has mainly been operated at field settings corresponding to momenta of nominally 4 and 8 GeV/c $\pm 20\%$. Two angular settings of 44 and 129 mrad provide coverage in transverse momentum up to 1.5 GeV/c.

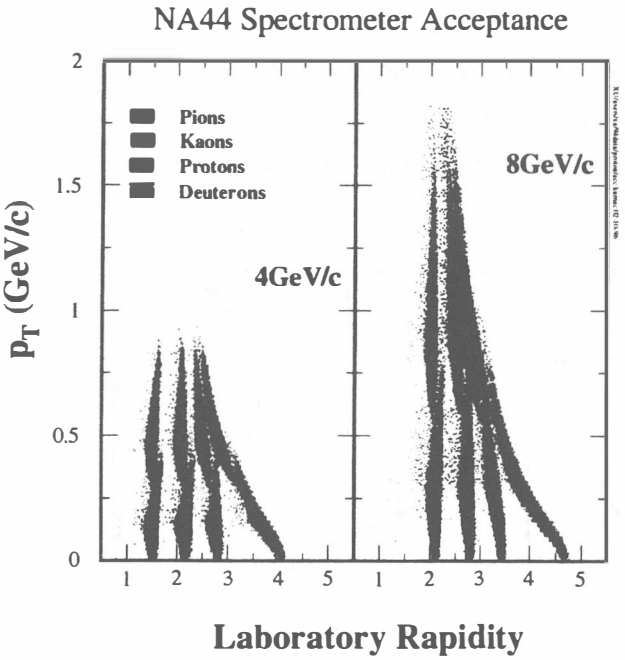

Figure 2: Acceptance of the NA44 spectrometer for pions, kaons, protons and deuterons.

3 Protons: Stopping at SPS energies

A central issue to be explored in heavy ion physics at SPS energies is the degree of nuclear stopping achievable in collisions between two Pb nuclei. This determines the transfer of kinetic energy from the beam to the internal degrees of freedom of the fireball, and fixes the initial conditions of the hot and compressed central collision zone. The degree of stopping may be inferred from the measured rapidity shift of baryons belonging to the overlap zone of the colliding nuclei. Indeed, if stopping were complete, as is the case for low energy nuclear collisions, all baryons would be found at the rapidity of the center of mass after the collision (approximately 2.9 at SPS energies). If nuclei were fully transparent to each other the final rapidity distribution of baryons would reflect the inital rapidity

distribution, now with the two colliding nuclei receeding from each other. In the intermediate case, a measure of the amount of stopping is given by the shift of the average of the rapidity distribution (in one half of the full range) after the collision as compared to the average before the collision [3].

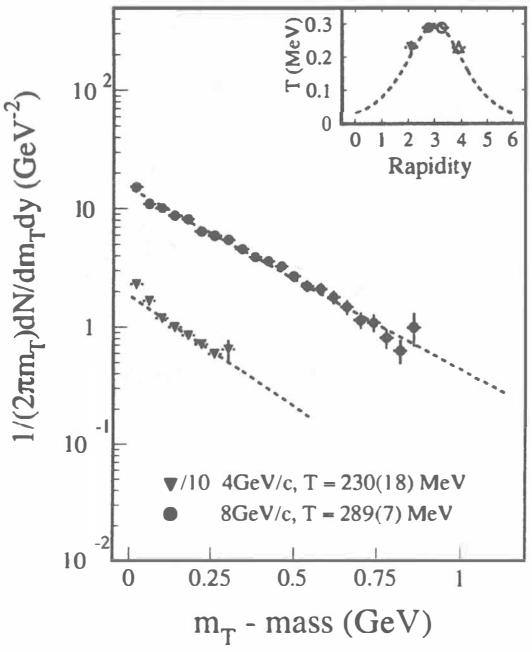

Figure 3: NA44 proton transverse momentum distributions for 4 (triangles) and 8(dots) GeV/c settings. The 4 GeV/c points are downscaled by a factor of 10 in the figure. Fitted slope parameters are indicated. The dashed line in the inset shows the function $T/cosh(y)$ with $T = 0.3GeV$, and the fitted slope parameters.

Figure 3 shows measured invariant cross sections for protons, measured by NA44, and plotted as a function of tranverse mass [2]. The distributions are shown for two rapidity regions and correspond to central collisions, defined as 15% of the geometric cross section. By fitting these distributions to an expo-

nential function and extrapolating beyond the measured region, the total proton multiplicity for the considered rapidity interval is obtained. Figure 4 shows the corresponding dN/dy distributions as a function of rapidity y. The data points in figure 5 have been reflected around midrapidity, which is a legitimate procedure for symmetric collisions. In the figure, the data are compared to predictions from two microscopic cascade models. It may be noted that the measured distribution appears to be intermediate to the Fritiof model (which does not contain significant nucleonic rescattering) and the RQMD model (which has significant rescatter and thus describes large stopping). The average rapidity shift that may be calculated from the experimental data under reasonable assumptions about the full rapidity distribution is $dy = 1.7$. This tendency has been observed also by the NA49 experiment as reported at this conference by Foka and in [6]. In similar AGS experiments for Au at 11.6 GeV.A on Au [8], a rapidity loss of $dy = 1.02$ is found. A simple rapidity scaling of dN/dy distributions and of the associated mean rapidity shifts would predict a rapidity shift of about 1.8 at CERN energies which together with the shape of the dN/dy distribution suggests that maximum stopping is reached between AGS and CERN energies. This result is of significance for predicting the amount of stopping that we may anticipate at higher energies, e.g. at RHIC energies.

4 Temperature, flow and thermalization

Single particle hadron spectra, not only provide information on particle yields of different species but also contain information on detailed properties of the emitting source, such as its temperature and expansion velocity.

While the slopes of transverse single particle spectra directly reflect the temperature of the emitting system if it is in thermal equilibrium and expanding freely (evaporating), the situation is more complicated in the presence of significant compression of the source. Indeed in this case there is an additional

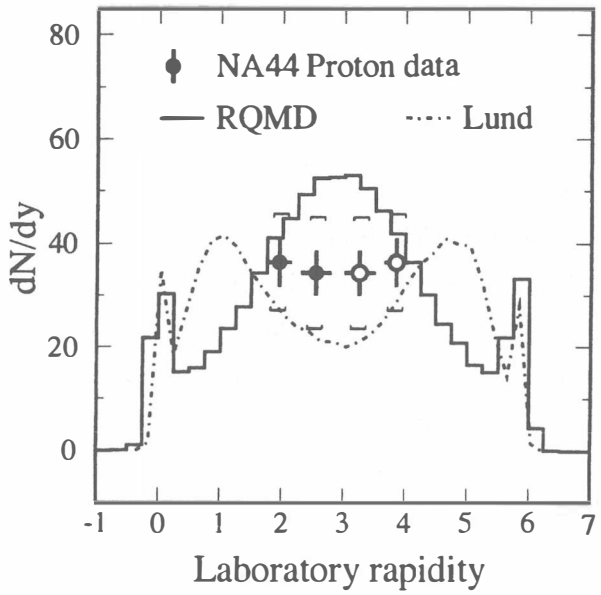

Figure 4: Proton rapidity distributions from central Pb+Pb collisions ($\sigma_{trig}/\sigma \approx$ 6%. Open circles are mirrored around $y_{mid} = 2.9$. Systematic errors are shown by vertical brackets. Solid and dashed lines are model calculations.

pressure component that contributes to an outward flow of the matter. This effect is directly observed in transverse NA44 single particle spectra at SPS energies [7]. Figure 5 shows the systematics of distributions for π^+, K^+ and p (left) and π^-, K^- and $\bar{p}$ (right) as a function of $m_t - m$. Comparison shows no significant difference between measured inverse slopes for negative and positive particles of a given kind. A systematic trend is however apparent when comparing inverse slopes for particles of different mass, as summarized in figure 6. Heavier particles have larger inverse slopes. A naive understanding of this effect follows from considering the total energy of a particle from the source. This may in the most

simple approach be written as the sum of the thermal energy and the kinetic energy arizing from the pressure driven expansion. Considering only transverse components of the expansion

$$T = T_0 + m < v_t >^2 \tag{1}$$

where T is the apparent temperature, T_0 the freeze-out temperature and v_t the transverse expansion velocity. Modifications to this expression arize if the hydrodynamical flow is considered in more detail /citeCsorgo. However, this simple expression is regained if the matter expands in a self similar fashion (i.e. like a Hubble expansion).

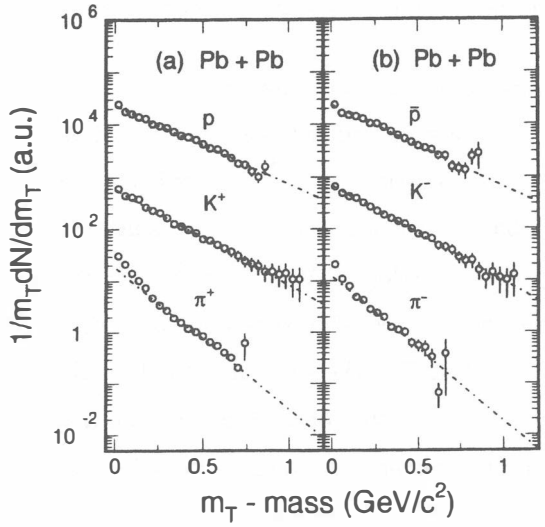

Figure 5: Transverse mass distributions for pions, kaons and protons from Pb+Pb central collisions measured in NA44. Dashed lines represent the exponential fits.

In any case one might expect that inverse slopes of spectra for particles of vanishing mass would approach the true temperature of the source, as indeed would be the case for photons. It is noteworthy that the systematics of inverse slopes shown in figure 6, for different types of reactions, all converge towards a

single value around T= 140 MeV as the considered particle mass decreases.

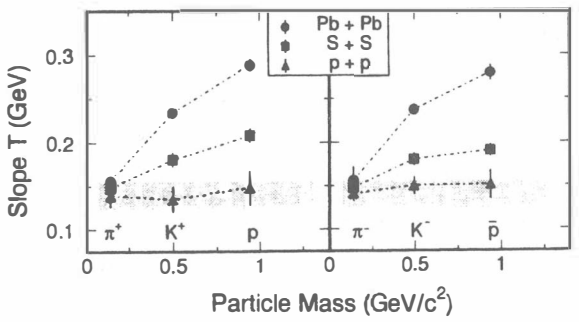

Figure 6: Slope parameter T as a function of particle mass. The shaded band shows the range where the slopes converge at zero mass. NA44 data.

Similar analyses have been done for data from Au + Au collisions at the AGS at 11.6 GeV/c. There a very similar value of the 'intrinsic' temperature is obtained. Systematics of temperatures as a function of beam energy in heavy ion collisions at lower bombarding energies show an increasing trend in contrast to the 'plateau' that appears to develop at AGS and SPS energies.

At the present time one may speculate as to the reason underlying this 'saturation': i) it may be "accidental" in the sense that it reflects the temperature of the system at freeze-out, i.e. at a later stage of the reaction than the initial and perhaps hotter phase, ii) it may reflect the so-called Hagedorn temperature which arises as a limiting temperature because at around this temperature it becomes advantageous to create pions rather than increasing the temperature or iii) it may reflect that the temperature of the system does not increase further because additional energy transfer is used in latent heat (phase transition scenario). To choose among these various possibilities is not so easy at present, not least because of the unhappy coincidence of the value of the pion mass and the value of the expected critical temperature of QCD.

5 Pion ratios as probe of expansion dynamics

It turns out that ratios of particle spectra may also be used to constrain parameters describing the particle emitting source. In a recent model analysis [13] of the ratio of spectra of negative pions and positive pions measured in NA44 [1], we find sensitivity to the freeze-out temperature, transverse expansion velocity and freeze out time of the source.

The effect may be simply understood: due to Coulomb forces π^- are decelerated in the field of the (positive) source, while π^+ are accelerated. This results in an increase in the π^-/π^+ ratio at low transverse momenta. The ratio is sensitive to the tranverse expansion velocity of the source since a fast expansion rapidly dilutes the positive charge of the source thus reducing the importance of Coulomb effects.

In the model [13] we assume that the pions can be described by a thermal distribution (characterized by a temperature T) that is superimposed on a collective outward flow of the matter described by a 4-velocity field u^μ

$$u^\mu = (\gamma_\perp \cosh y', \gamma_\perp \sinh y', \mathbf{u}_\perp), \quad \gamma_\perp = \sqrt{1+\mathbf{u}_\perp^2}, \quad \mathbf{u}_\perp(r) = \frac{\bar{\beta}}{\sqrt{1-\bar{\beta}^2}} \frac{\mathbf{r}_\perp}{R}. \quad (2)$$

This field describes slices which move with rapidity y' in longitudinal z-direction (i.e. along the beam axis). We assume that the reaction zone has an axially symmetric cylindrical shape and that the the transverse 4-velocity $\mathbf{u}_\perp$ scales linearly with the radial distance $\mathbf{r}_\perp$ from the axis. The transverse velocity $\bar{\beta}$ describes the motion of a characteristic radius R.

Assuming that the particles are distributed over the rapidity slices as a Gaussian distribution centered at the center-of-mass rapidity y_{cm} the pion source distribution at freeze-out is

$$\frac{d^6N}{dyd\mathbf{p}_\perp^2 dzd\mathbf{r}_\perp^2} \sim \int dy' \exp\left[-\frac{(y'-y_{cm})^2}{2\Delta y^2}\right] \delta(z-\tau_f \sinh y') F(\frac{r_\perp}{R}) \times \frac{u_\mu p^\mu}{\exp(u_\mu(p^\mu - eA^\mu)/T) - 1}, \quad (3)$$

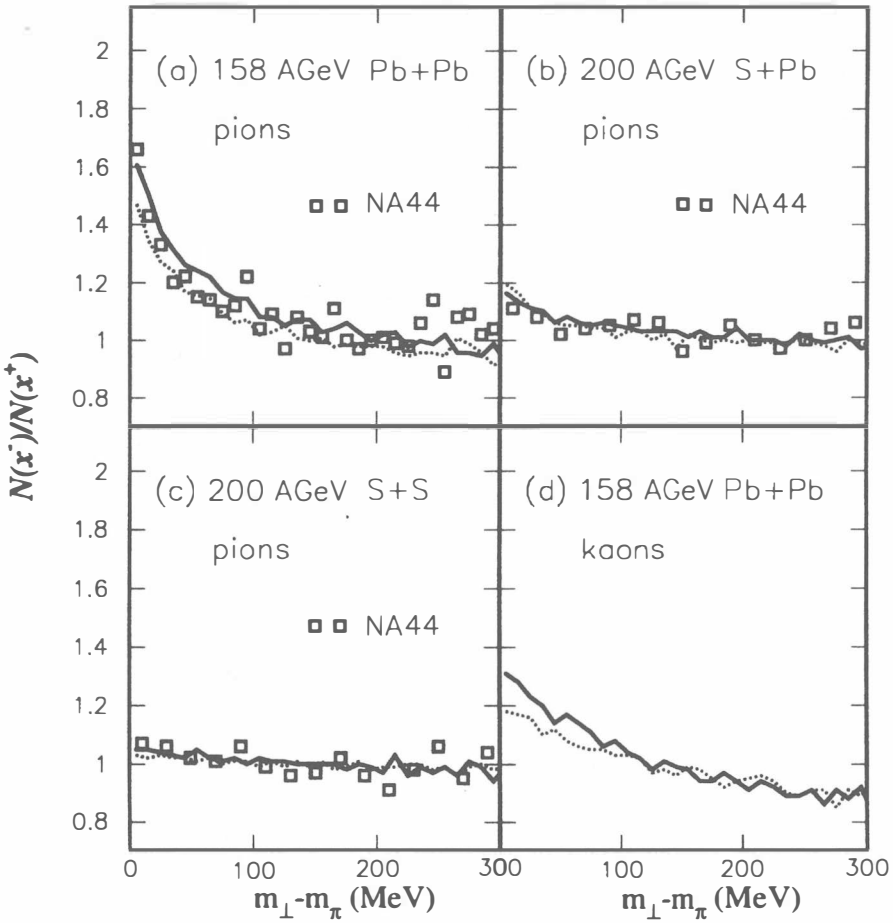

Figure 7: Experimental π^-/π^+ ratios for the reactions (a) Pb+Pb, (b) S+Pb, and (c) $S+S$ as a function of transverse mass compared to calculations (solid lines) using the dynamical Coulomb model with a best-fit freeze-out time of 7 fm/c. The dotted lines show the results for a detector located exactly at midrapidity. Panel (d) shows the predicted arbitrarily normalized K^-/K^+ ratio for the Pb+Pb reaction.

where p^μ, e, and A^μ denote the pion momentum and charge and the electromagnetic 4-potential of the source, respectively. The distribution is a function of the rapidity y, the transverse momentum $\mathbf{p}_\perp$, and the longitudinal and transverse extensions z and $\mathbf{r}_\perp$. In the spirit of the Bjorken picture the longitudinal distance z is related to the rapidity y' of the cells via an effective freeze-out time τ_f although in reality there will be a distribution of freeze-out times. The width Δy is taken from experiment.

The subsequent motion of the pions in the expanding electromagnetic field created by the net charge is described by the 4-velocity w^μ which satisfies the equation of motion in the electromagnetic potential A^μ

$$m\frac{d}{d\tau}w^\mu = ew_\nu(A^{\nu,\mu} - A^{\mu,\nu}), \tag{4}$$

where τ denotes the proper time and m is the pion mass. The final spectra are obtained by sampling over a set of different initial conditions using eq. (3).

Figure 7a-c shows a comparison of the calculations to NA44 experimental data for $Pb + Pb$ collisions at $E = 158AGeV$ and for $S + Pb$ and $S + S$ at $200AGeV$ [1], all for central collisions and rapidities $3.3 < y < 4.0$. The calculations take the actual NA44 detector acceptance (figure 2) into account. In addition, we also plot calculations corresponding to a detector located exactly at midrapidity. Calculated ratios are normalized to unity in the region $200MeV < m_t - m_\pi < 400MeV$, as is done for the experimental results.

The NA44 lead data were taken with a trigger selecting 15% of the total interaction cross section. In a sharp cut-off model this implies an average charge of $Z_{cent} = 122$ in the fireball. In the calculations the charge of the participant zone is fixed to this value. We transform the transverse area into a circle of $R_{geom} = 5.8$ fm. At freeze-out we take a radius of $R = R(\tau_f) = R_{geom} + \bar{\beta}\tau_f/2$ assuming the linear increase of the transverse velocity. The widths of the pion rapidity distributions was chosen to be $\Delta y = 1.3$ according to measurements in $S + S$, $S + Pb$ [5] and with measured transverse energy spectra in $Pb + Pb$ collisions[6].

We use a temperature of $T = 120MeV$ and $\bar{\beta}$= 0.62 corresponding to a mean transverse expansion velocity $\langle\beta\rangle = 0.42$. These parameters agree with the values obtained from the analysis of measured transverse π, K and p spectra from $Pb+Pb$ discussed in the previous section [7]. The dN/dy vs y data from the NA44 experiment [2] and recent similar data from the NA49 experiment [4] provide double-humped rapidity distribution of protons which can be characterized by the parameters $\Delta y_{ch} = 0.84$ and $y_1 = 1.1$, implying a rapidity loss of 1.7. Here, $y_1 = 1.1$ is the centroid difference between the two bumps and $\Delta y_{ch} = 0.84$ is the width of each component.

Using these values a good description of the experimental data (see Fig. 7a) is obtained using a freeze-out time of 7 fm/c. Figs. 7b and 7c show a comparison for lighter systems. Here we use a higher temperature of 130 MeV and a smaller velocity $\langle\beta\rangle = 0.29$ [5, 10]. A fit to the $S+S$ data [5] indicates a smaller rapidity loss of 1.3, leading to $\Delta y_{ch} = 1.25$, $y_1 = 1.7$. For the asymmetric $S+Pb$ reaction a good description of the data is obtained (see Fig. 7b) by assuming that 30 protons from the Pb target and all protons from the projectile participate in the fireball decelerated to their respective rapidities y_1.

The effect of varying the various parameters is exhibited in Fig 8. The magnitude of the enhancement scales with the total participant charge and diminishes if the charge is distributed over a wider rapidity range (Fig. 8a). If the system expands fast, the slower pions are overtaken by the expanding potential and experience a smaller net charge. Faster expansion can be due either to increasing collective flow (Fig. 8b) or larger thermal motion (Fig. 8c). In either case a reduction of Coulomb effects results. A stronger effect is observed when the formation time τ_f increases, see Fig. 8d, reflecting a more diluted charge distribution.

The model analysis depends significantly on the freeze-out time. Hanbury-Brown and Twiss (HBT) analysis provides two independent comparisons of this time. In a longitudinally expanding system with Bjorken scaling the freeze-out

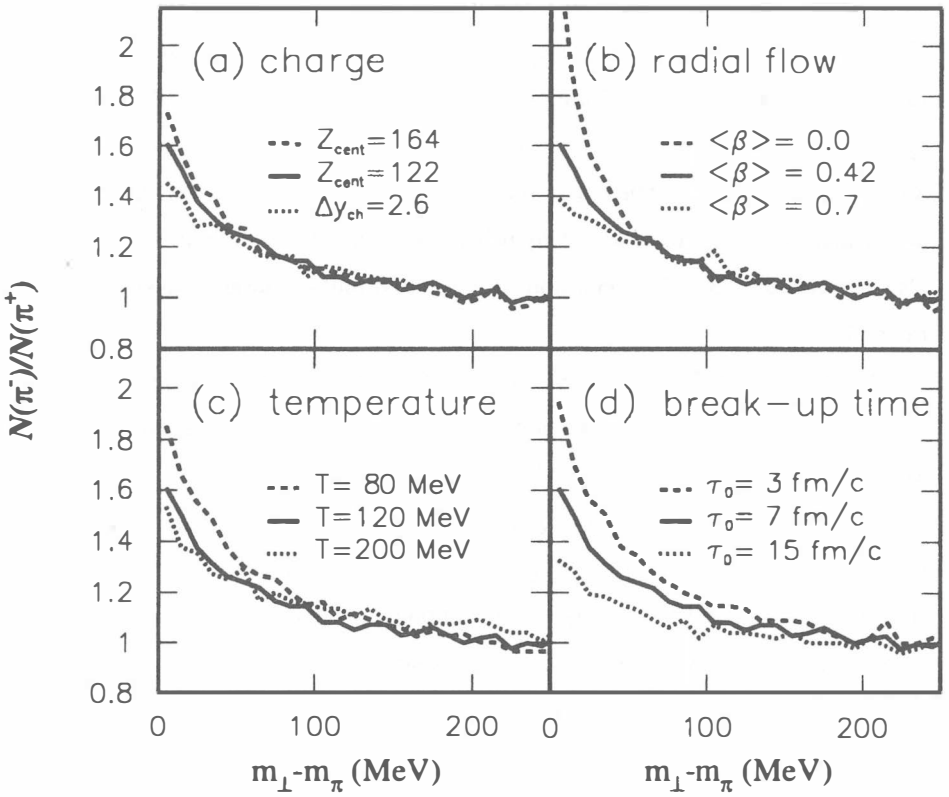

Figure 8: Comparison of the sensitivity of the calculations to variation of the main parameters. Solid lines represent the best fit calculations for the $Pb + Pb$ reaction shown in Fig. 1. Variation of : (a) total participant charge Z_{cent} and width of rapidity distribution, (b) average transverse expansion velocity $\langle\beta\rangle$, (c) temperature at freeze-out, (d) freeze-out time τ_f.

time is related to the longitudinal HBT radius by $\tau_f = R_l \sqrt{m_\perp/T}$. From the NA44 data $R_l \simeq 5.5$fm [11] we estimate $\tau_f \simeq 8$fm/c. From transverse HBT radii we obtain $R = 2R_s \simeq 10$fm. Comparing to $R = R_{geom} + \bar{\beta}\tau_f/2$ we deduce $\tau_f = 8$fm/c; this value should, however, be corrected for transverse flow which also affects the HBT radii. Thus both freeze-out times extracted from the longitudinal and transverse HBT radii are compatible with that obtained from π^-/π^+. We also remark that RQMD calculations predict substantially larger values of τ_f=15 fm/c [12].

The calculated kaon ratio K^-/K^+ in $Pb + Pb$ collisions, using the same parameter set as used for the pions, is shown in figure 8d. As the kaon is heavier we expect the corresponding K^-/K^+ ratio to be smaller.

It is worth noting that the magnitude of the Coulomb effects in pion spectra is sensitive to the degree of stopping and the resulting distribution of the positive charge. At RHIC and LHC energies the stopping and in particular the net charge at midrapidity are expected to be smaller, and consequently one would predict correspondingly smaller Coulomb effects.

6 The BRAHMS experiment at RHIC

In a just few years from now, it will be possible to study collisions between heavy ions with energies per nucleon pair of 200 GeV/c. It is expected that the amount of stopping will decrease as compared to present day CERN-SPS energies, continuing the trend in the dN/dy proton distributions as discussed in section 3. This may result in a separation of the particles that will be observed in experiment into two regions: a central region (midrapidity) where a volume with deconfined quarks and gluons (and vanishing net baryon density) may be created and a region at large rapidities where emission from the highly excited fragments will take place. Figure 9 shows predictions for particle production at RHIC calculated with three models with different amounts of stopping. It is obvious

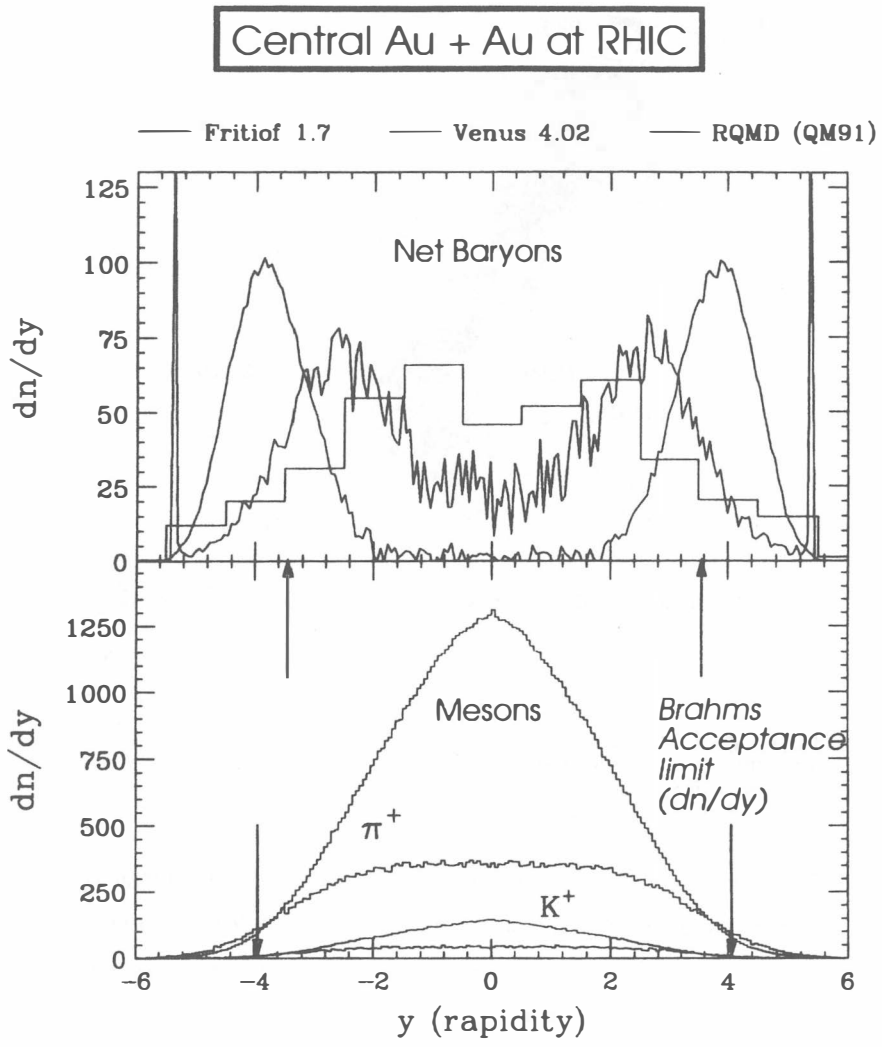

Figure 9: The dn/dy distributions predicted for Au+Au collisions at RHIC energies within various models. The BRAHMS rapidity acceptance is indicated.

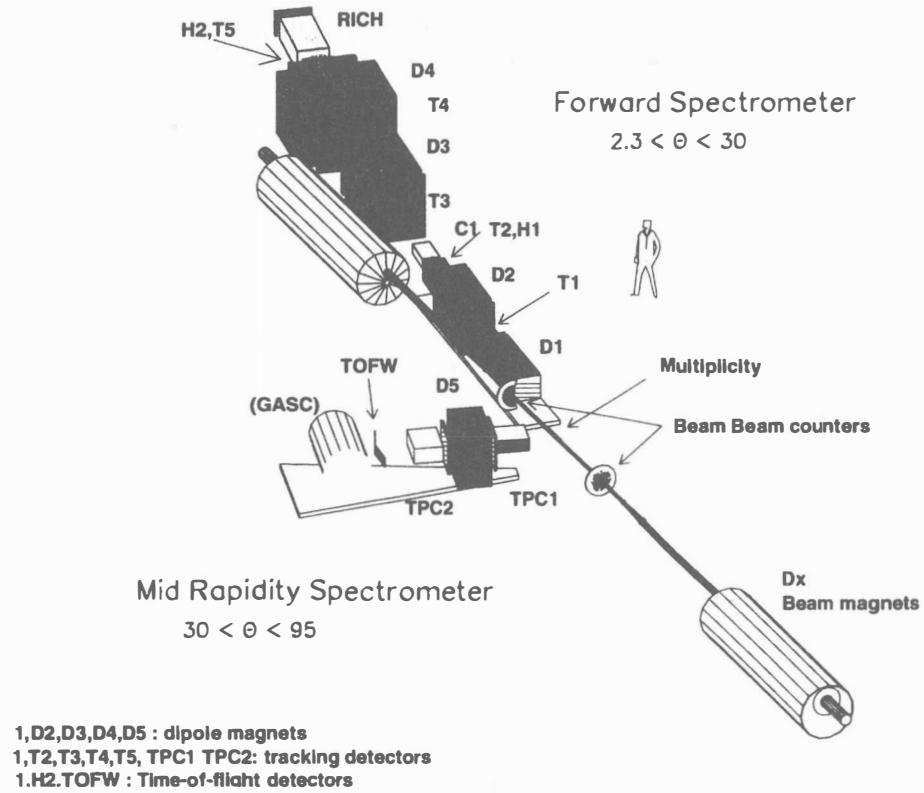

Figure 10: The BRAHMS experiment for RHIC consist of two magnetic spectrometers capable of covering the angular range from 2.3 degrees to 90 degrees, corresponding to a rapidity coverage for identified charged hadrons from 0 to 3.5.

that a RHIC it will be important to cover a large rapidity range in particular if it turns out that the separation is not complete. One of the four RHIC experiments, namely the BRAHMS (Broad Range Hadronic Magnetic Spectrometer) detector, shown in figure 10, will have the capability of covering a rapidity range from 0 up to 3.5 with full identification of charged hadrons up to high momenta. The BRAHMS detector which is now fully approved for construction is a collaboration between groups from the USA (BNL, Kansas, Texas, NYU, SSL) and Europe (NBI, Bergen, Oslo, Strasbourg and Krakow).

7 Conclusions

NA44 data from central $Pb + Pb$ collisions at $158 AGeV$ show the presence of significant nuclear stopping at SGS energies, although there are indications that maximum stopping is reached at energies between the present AGS and SPS regime. This sets the scene for significant compression and heating of the nuclear matter.

Transverse single particle spectra of pions, kaons and protons provide evidence that matter at the SPS flows outwards due to a significant pressure gradient. A systematic analysis of spectrum slopes suggests that the average transverse expansion velocity is around 0.4c and that the freeze-out temperature is around 140 MeV.

An independent analysis of the ratio of π^-/π^+ at low transverse moementa substantiates these findings. The observed enhancement of the π^-/π^+ can be explained as resulting from the Coulomb acceleration of the pions by the positive charge in the expanding system. A quantitative model analysis, assuming thermal equilibrium of the expanding matter, yields expansion velocities that are consistent with the analysis of the single particle spectra. A freeze-out temperature of 120 MeV and a charge freeze-out time of 7 fm/c are deduced.

The support of the Danish Natural Science Research Council is appreciated.

References

[1] H. Bøggild et al., NA44 collaboration., Phys. Lett. **B 372**, 343 (1996)

[2] I. G. Bearden et al., NA44 collab., Phys. Lett. **B388** (1996) 431

[3] F. Videbæk and O. Hansen. Phys. Rev. C52 (1995) 2684.

[4] T. Wienold for NA49 collab., Quark matter '96, Proc. of the 12th Int. Conf. on Ultra-Relativistic Nucleus-Nucleus Collisions, Heidelberg, Germany, May 20-24, 1996

[5] D. Röhrich et al., NA35 collaboration, Nucl. Phys. A566, 35c (1994); J. Bächler et al., Phys. Rev. Lett. **72**, 1419 (1994)

[6] T. Alber et al., Phys. Rev. Lett. **75**, 3814 (1995).

[7] I. G. Bearden et al., Phys. Rev. Lett. **78** (1997) 2080.

[8] M. Gonin. Nucl. Phys**A566** (1994) 601c.

[9] T. Csörgö and B. Lörstad. Phys. Rev. **C54**(1996) 1390.

[10] P. Braun-Munzinger et al., Phys. Lett. **B 365**, 1 (1996)

[11] A. Franz for NA44 collaboration., Quark matter '96, I. G. Bearden et al., Nucl. Phys. A610 (1996) 240.

[12] H. Sorge, Phys. Lett. **B373**, 16 (1996)

[13] H.W. Barz, J. Bondorf, J. J. Gardhøje, H. Heiselberg, Phys. Rev. C. (1997). In press.

[14] BRAHMS Conceptual Design Report. BNL-62018.